TheATLAS

Safe Room Wall Design for Tornado Survival

[1] ***Melisa A. Blahnik,*** [2] ***Emrah Gumus,*** [3] ***Bobby G. McPeak, and*** [4] ***Atila Ertas*** [1] *Briggo Inc., Austin Texas, Email: melisa.blahnik@gmail.com;* [2] *Aselsan, Defense & Space, Ankara, Turkey, Email: emrahgumus@aselsan.com.tr;* [3] *Raytheon Company, Dallas, TX 75243, USA, Email: mcpeak@raytheon.com;* [4] *Texas Tech University, mechanical Engineering Department, Lubbock, Texas, Email: aertas@coe.ttu.edu*

doi: 10.22545/2014/00048

A safe room is a reinforced structure specially designed to meet the Federal Emergency Management Agency (FEMA) criteria and provide protection in extreme weather events, including tornadoes and hurricanes. The materials used for safe room walls are expected to resist loads imposed and tornado debris impact. Tornadoes rated as high as EF-5 can create maximum wind speeds of more than 300 mph, which is enough to demolish any structures in their path. These maximum wind speeds produce forces that are about twice as large as those produced by the strongest hurricanes. One of the common safe room wall designs is made of plywood/steel-plate composite. The main objective of this paper is to use a finite element simulation code, LS-DYNA, to predict the dynamic response of plywood when impacted by tornado missiles such as 2 x 4 wood timbers.

Keywords*:* Tornado, debris, Impact, simulation.

1 Introduction

The safe room project is part of a continuing FEMA initiative named Project Impact: Building Disaster Resistant Communities designed to urge people and communities to take measures to protect themselves and their property before disasters occur.

Throughout history tornadoes have signified a force of nature that is both admired and feared. Tornadoes tend to strike with little warning, without regard to season, and just as quickly they are gone. The result is often devastating in terms of property damage and the human toll. Until recently, the fundamental knowledge of tornado behavior escaped explanation. As our understanding of tornadoes advances, it is more evident than ever that tornadoes are not magical entities. They are natural phenomena that follow the laws of physics, and as such are excellent subjects of deep research. Most of the research regarding the tornado belongs to the atmospheric sciences, but this status is experiencing a change. With the introduction of engineering into the sphere of tornado research, a new paradigm is changing the way that the world looks at these natural wonders.

While tornadoes occur in different parts of the world, the highest concentration of tornadoes occur in the United States [1]. Approximately 1,200 tornadoes per year strike the United States; more than any other nation in the world. According to the National Climate Data Center from 1953 through 2005, there were 48,632 reported tornadoes in the United States, resulting in 4,388 deaths [2]. The most devastating tornado in recorded history took place in 1925. The path of this tornado (or possibly a family of

Figure 1: Automobiles are no match for 200+ mph winds [4].

Figure 2: The original location of these automobiles are unknown [4].

tornadoes) extended through Missouri, Illinois, and Indiana. During the 219-mile track (at times 1200 yards wide with a forward speed of up to 72 miles per hour), 695 people were killed, 13,000 injured, and caused $17 million in property damage [3]. This tornado stayed on ground for 3 hours. Though tornadoes do not represent the greatest threat against life in the United States, they embody a particularly disturbing hazard.

Debris is a hidden danger in tornado. People can be easily injured by flying debris. One of the strongest tornadoes, rated an EF-4 ripped though the Union University campus in Jackson Tennessee in 2008. The damage at Union University was severe. Automobiles became debris and some of the dormitories suffered catastrophic damage (see Figures 1 and 2) [4].

The materials used for safe room walls are expected to resist loads imposed and tornado debris impact. Tornadoes rated as high as EF-5 can create maximum wind speeds of more than 300 mph, which is enough to demolish any structures in their path. These maximum wind speeds produce forces that are about twice as large as those produced by the strongest hurricanes. The main objective of this paper is to investigate the performance of safe room wall assemblies when subjected to the impact and penetration of windborne debris.

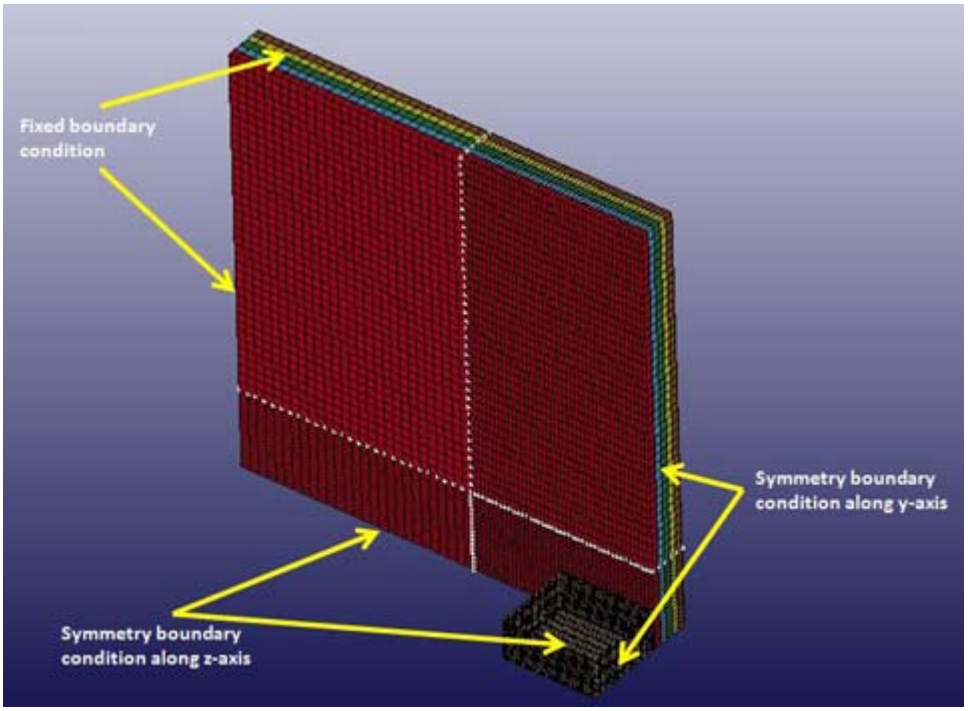

Figure 3: Boundary Conditions.

2 Penetration mechanics

Widespread research exists on penetration problems by many researchers to develop fundamental relationships applied to areas such as hypervelocity impact, shaped-charge penetration, long-rod penetration, small arms, ballistic protection, and armor design. The basic understanding of penetration mechanics is as follows. Given a projectile, a target, and details of the initial geometry, kinematics, and materials properties; investigate whether or not target perforation occurs. If perforated, investigate what the residual characteristics of projectile and target will be, and if not, investigate the depth of penetration.

Penetration mechanics is one of the most involved problems in the research field of mechanics, and researchers have been working on the solutions many years. Solution approaches exist on three different levels as follows [5]:

- Data correlation
- Engineering models
- Numerical simulation

Many research works have occurred, resulting in satisfactorily accurate simulations of penetration problems [6, 7, 8, 9, and 10]. Zukas and Anderson reviewed the state of the art of numerical simulations which describes the impact and penetration mechanics including a comprehensive review [11]. They examined the general capabilities and limitations of numerical simulations. They stated that as the size and speed of computers have increased so has the complexity of codes used for these purposes; but certain characteristic difficulties persist [12].

3 Modeling

Composite materials have been used widely in many applications such as in the oil industry, space structures, pressure vessels, and automobile industries. Many researchers have investigated a solution to the impact on composite laminates using finite element method [13, 14, 15, 16].

Plywood is a layered, cross-ply, unidirectional, fiber-reinforced composite. Plywood strength and progressive failure resistance are important for the survivability of house frames when earthquakes, tornados, and/or hurricanes occur. Plywood is made of thin sheets of timber called plies. The plies are cut by rotating the trunks then stacking them together with the fiber direction of each ply perpendicular to the fiber direction of its adjacent ones. The plies

Table 1: Rigid Material Properties.

Material Parameters of the Projectile Units (kg, mm, ms, kN, Gpa)		
Ro	Mass Density	5.272E-005
E	Young's Modulus	16.719
PR	Poissons's Ratio	0.365

are bonded using strong adhesive under heat and pressure. In general, plywood has an odd number of plies [17].

One of the common safe room wall designs is made of plywood/steel-plate composite. In this research, numerical simulation LS-DYNA analysis code predicts the dynamic response of plywood when impacted by tornado derbis such as 2 x 4 wood timbers will be used. Due to the differences in speed between the types and classes of wind events, specific criteria were developed to simulate the results of such an impact event.

In this paper, the LS-DYNA analysis code is used to identify the damage of the composite plywood impacted by a rigid projectile. Because of the symmetry of the problem, only one quarter of the geometry is modeled. In this case, the plywood is assumed to be five layers of composite material. In order to reduce the computational time while keeping the inertia of projectile same as 15 lb 12 ft 2x4 wood timber, a 1.5 inch projectile was used. The projectile was assumed to be rigid and the target (3/4 plywood) assumed to be elastic-plastic material. In modeling, solid elements were used because of the ease of use and better stability of contact problems (Chatiri, Gull and Matzenmiller n.d.). Each layer of the target is 8" x 8" x 0.15" and the projectile dimensions are 1.75" x 0.75 x 1.5". The density of the projectile arranged such that the projectile part has a weight of 15 lbs.

The projectile and the target are discredited by 8-node hexahedron solid elements, using only one integration point. The target has simulated 5 layers through the thickness. The impact region has a fine mesh with element size of 2.12mm x 2.12mm x 3.81mm for each layer. The transition region has an element size of 2.12mm x 4.23mm x 3.81mm, and the transition region's coarse mesh size is 4.23mm x 4.23mm x 3.81mm. The element size for the projectile is finer than that of the impact zone of the target which is 1.27 mm x 1.27mm x 3.81mm. Each layer of the target has 3933 brick elements therefore target has total 19665 brick elements. Projectile has 1818 brick elements.

As shown in Figure 3, two different kinds of boundary conditions are used because of the symmetry of the problem–fixed-boundary condition and symmetry-boundary condition. The symmetry boundary condition is applied on the bottom and right face of both the target and the projectile. The fixed boundary condition is applied on the model on the upper and left face of the target. The bonding between the plies is modeled with "contact tie break surfaces," which has the fracture-mechanics-based delimitation capability. The contact was defined between each ply, allowing them to delaminate from each other. Moreover, eroding contact surfaces are modeled to control the impact force between the projectile and the target. The most important factor of the contact surfaces is that it helps to redefine itself after an element fails and is removed from the model.

Material modeling – Material Model 20 "MAT-RIGID" is applied for modeling the projectile while Material Model 143 "MAT_WOOD_PINE" is applied for modeling the target layers. For this study, material model 143 is used for 10% moisture content. Table 1 shows the material properties of the projectile material and Tables 2-A, 3-A, 4-A, and 5-A (see Appendix) show the material properties of the target with 1%, 10%, 20%, and 30% moisture contents.

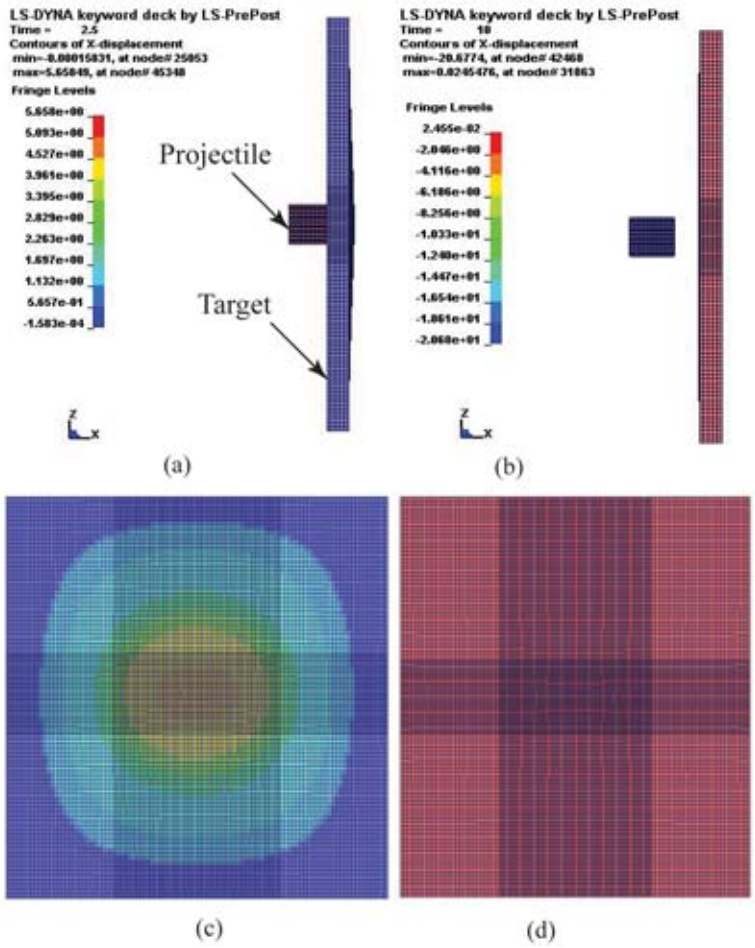

Figure 4: Composite plywood impacted by 4 m/s projectile.

4 Results and Discussions

In order to find the impact velocity that penetrates the composite plywood, velocities of 4m/s, 6m/s, 8m/s, 10m/s, 12m/s, 13m/s, 13.5m/s, 13.8m/s ,13.9m/s, 14m/s, 15m/s, 16m/s, 17m/s, 18m/s, 20m/s, 22m/s, 30m/s, 40m/s, and 45m/s with 10% moisture content plywood are simulated. Furthermore, 1% moisture content, 20% moisture content and, 30% moisture content plywood are also simulated with velocities of 13.5 m/s, 13.6 m/s, 13.8m/s, 13.9 m/s, and 14 m/s in order to record the difference resulting from various moisture contents.

To clarify the characteristics, side and back views of the simulation at 2.3 and 10 seconds are shown for only velocities of 4 m/s and 13.9 m/s at this time (see Figures 4 and 5). As seen in Figure 4, portraits (a) and (b) are the side views and portraits (c) and (d) are the back views of the simulation. Portraits (a) and (c) show the x-displacement at 2.5 seconds after the initial impact. Portraits (b) and (d) show the x-displacement at 10 seconds after the initial impact (the final configuration of the deformation). In some cases there was no deformation found after the impact and the projectile returns to the direction from which it came.

Identical simulation results are obtained until we reach the velocity of 13.9 m/s, meaning, deformation was elastic and no penetration was observed. However, as seen in Figure 5, penetration has occurred at velocity 13.9 m/s. It is clear from this figure that the penetrating projectile has extricated a solid block in the positive x-direction.

Penetration phenomenon is also evident from Figure 6(b). As shown in this figure, the projectile travels 13.9 m/sec in the positive x-direction and penetrated the target. Because there is no deflection in the x-direction, the rebound velocity no longer exists. Instead, a projectile has residual velocity. The projectile residual velocity is 1.22 m/s (9% of impact

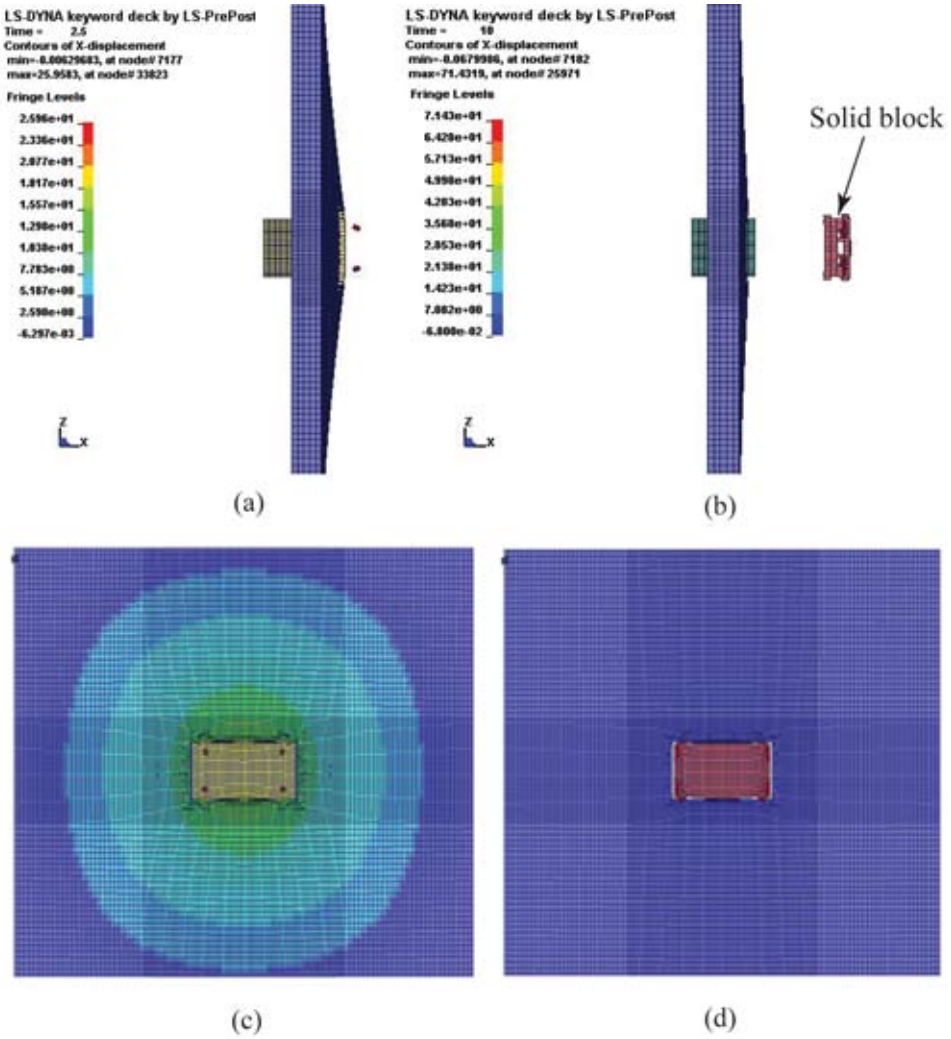

Figure 5: Composite plywood impacted by 13.9 m/s projectile.

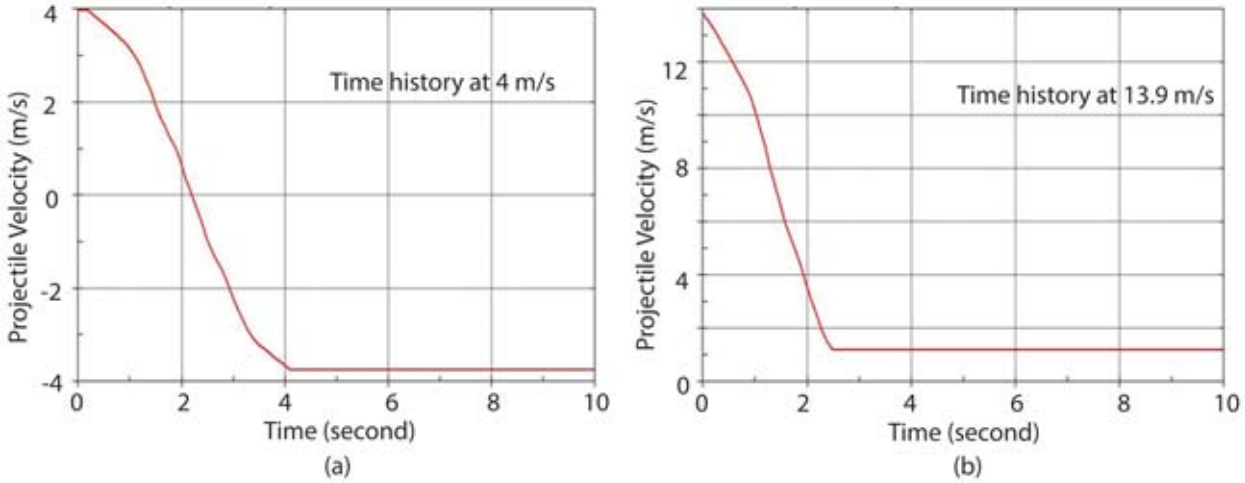

Figure 6: Projectile velocity vs. time history for 4 m/s and 13.9 m/s.

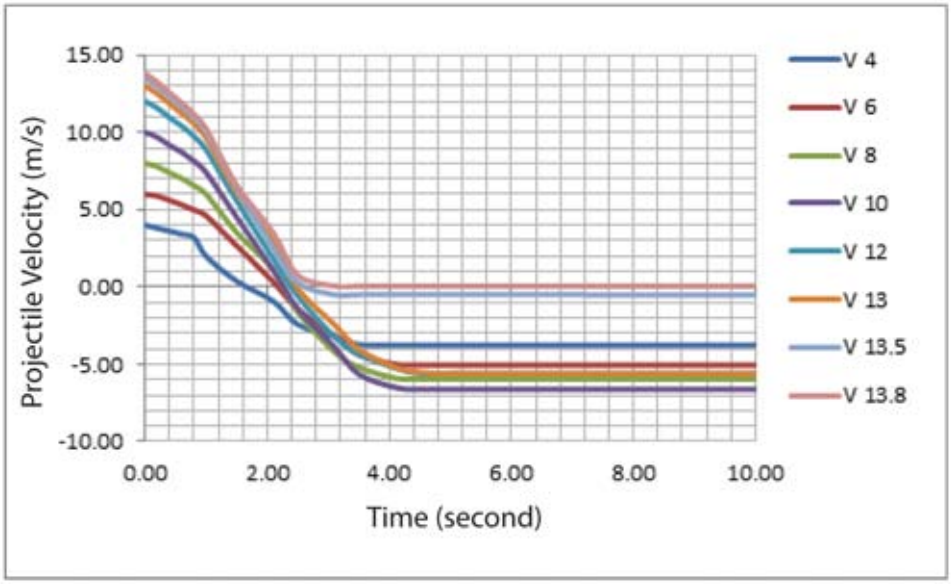

Figure 7: Projectile velocity vs. time history before the penetration.

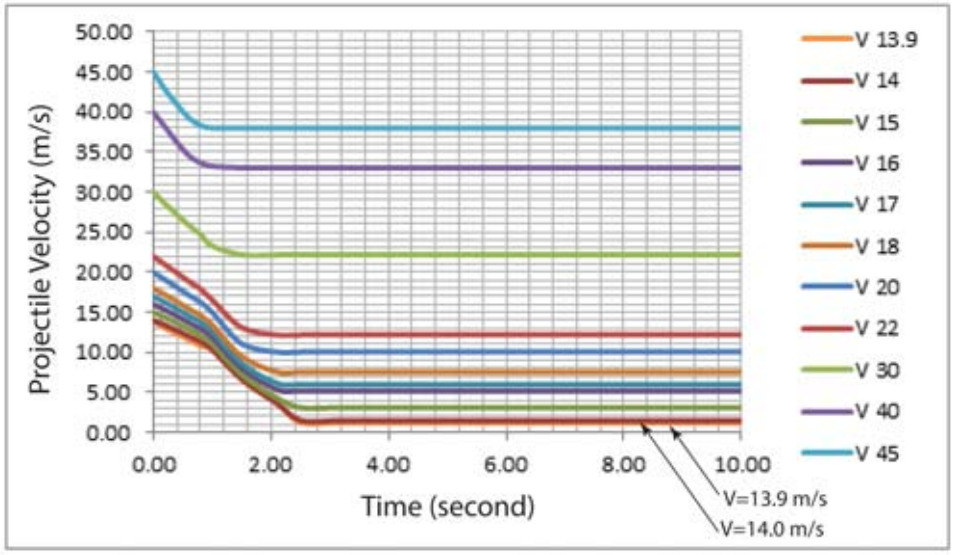

Figure 8: Projectile velocity vs. time history after the penetration.

velocity). This shows that the target absorbed most of the kinetic energy. As shown in this figure, the velocity remained in the positive region. As shown in Figure 6(a), the projectile travels at 4 m/sec in the positive x-direction and made contact with the target at which point the projectile and the target exchange energy – the projectile is deflected and travels in the negative x-direction with the rebound velocity of 3.75 m/sec. This makes the rebound velocity 94% of the initial impact velocity. This illustrates that the target absorbed very little of the kinetic energy from the impact. As shown in this figure, the transition of the velocity from positive to negative is exposed.

Figures 7 and 8 show the impact velocity profiles for all the velocities mentioned earlier. Figure 7 illustrates the first set of example. All the projectile impact velocities in this set fails to penetrate. As shown in this figure, rebound velocity occurs between 4 m/s and 13.8 m/s with the projectile deflecting in the x-direction (below zero) because of the energy exchange between the projectile and

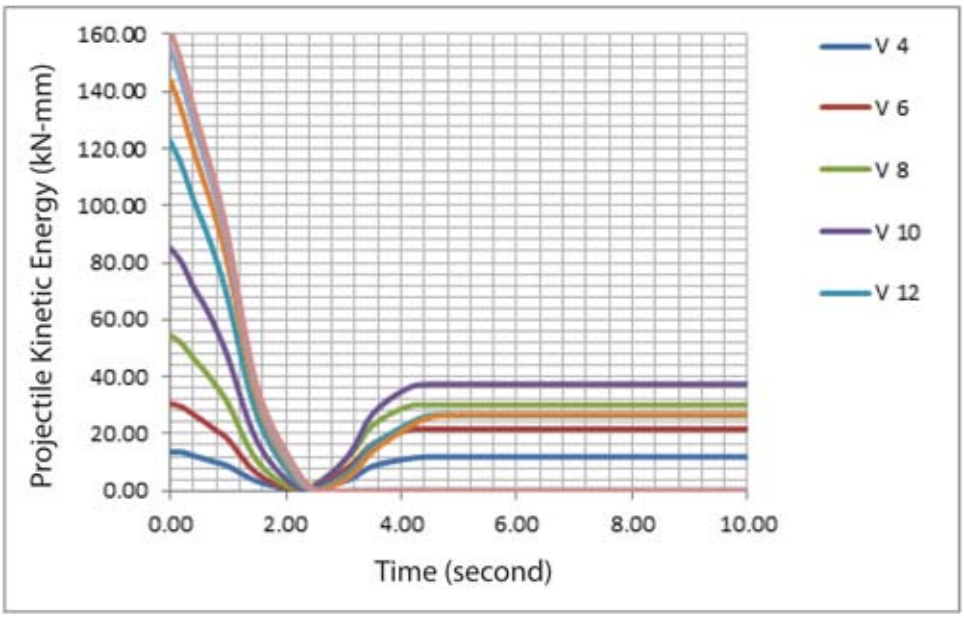

Figure 9: Projectile kinetic energy vs. time before the penetration.

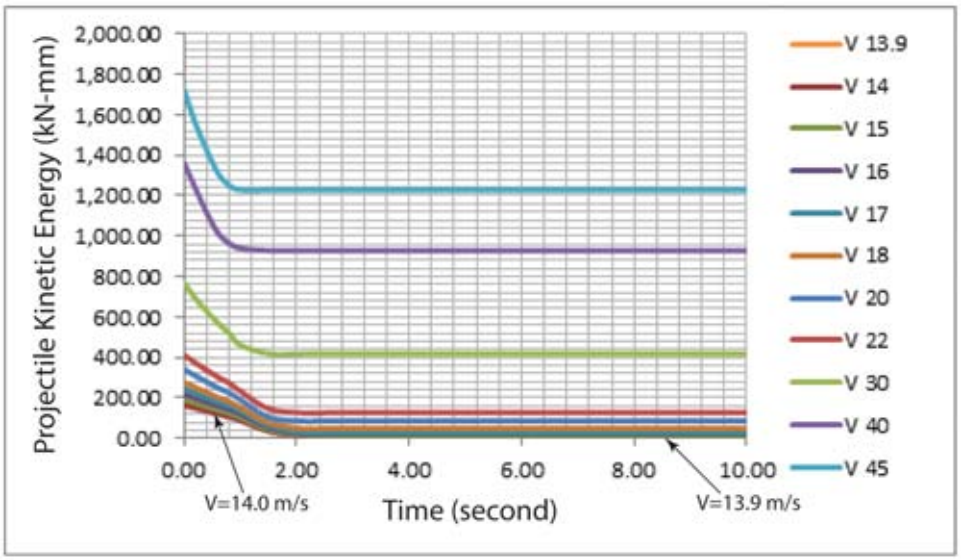

Figure 10: Projectile kinetic energy vs. time after the penetration.

the target. However, as shown in Figure 8, all the projectile impact velocities penetrate the target – residual velocity occurs between 13.9 m/s and 45 m/s with the projectile penetrating the target. Simulation at an impact velocity of 13.9 m/s is important as it predicts the limiting velocity for penetration. Texas Tech University test results indicate that the range of limiting impact velocity for penetration is between 13.2 and 14 m/s (29 and 31 mph). Note that since the simulation result at this impact velocity indicates that the remaining (residual) velocity is 2.75 m /s, the limiting velocity for penetration is somewhere below 14 m/s (31.3 mph). This is in reasonable agreement with the TTU experimental results.

Figures 9 and 10 illustrate the kinetic energy changes between projectile and the target (plywood). As shown in Figure 9, for example, when the projectile impact velocity is 4 m/s, the kinetic energy of the projectile decreased rapidly after the impact.

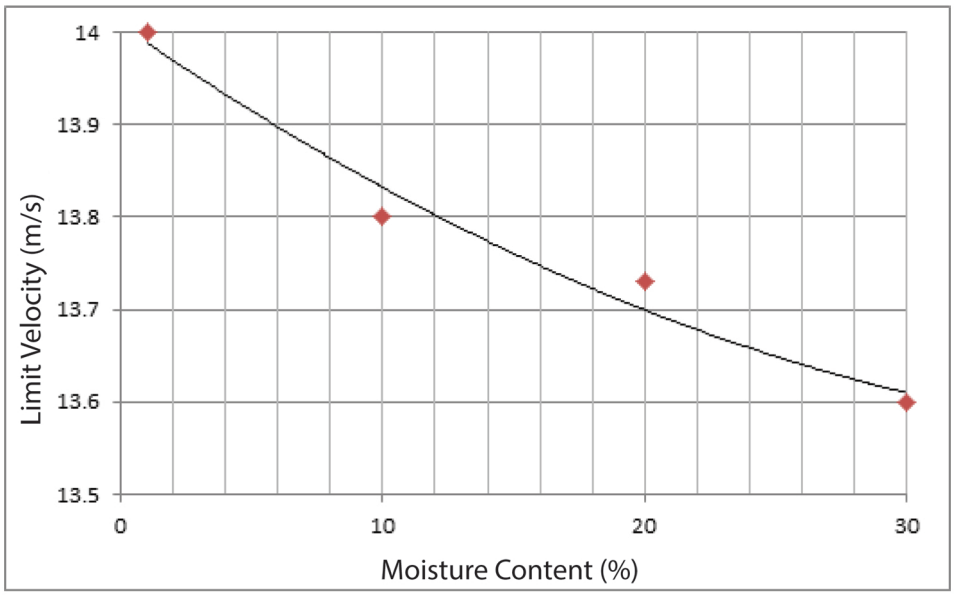

Figure 11: Limit velocity vs. moisture contents.

Since the projectile did not penetrate but changed direction, the velocity went to zero as the direction changed and then kinetic energy increased rapidly. However as shown in Figure 10, the kinetic energy of the projectile traveling at 13.9 m/sec decreased rapidly after the impact of the system. Since there is penetration, the target absorbed most of the energy – after the penetration projectile has almost zero velocity

Penetration limit velocity, V_L as mentioned earlier, is the minimum velocity level for penetrationof the projectile to embed in the target. In other words, when the projectile passes through the thickness of the target, remaining velocity becomes zero. For impacting velocities smaller than the penetration limit velocity, the projectile rebounds from the target. In this study, V_L-13.9 m/s is the limit velocity to penetrate one plywood. This value can also be verified by using following equation [1]:

$$V_L = \sqrt{\frac{R_t}{\gamma}(e^{2\alpha\gamma w} - 1)} \qquad (1)$$

Where R_t is the strength of the plywood (taget), w is the thickness of the target, and

$$\alpha = \frac{A}{m}; \qquad \gamma = \frac{1}{2}\rho_t \qquad (2)$$

Where m is the mass of the penetrator (projectile), A is the penetrator average cross-sectional area, and ρ_t is the density of the target. Using the data given in this paper, Eqn (1) provides limit velocity of approximately 14.3 m/s.

Figure 11 shows penetration limit velocity with respect to moisture content of the plywood. As seen from the figure, fully saturated wood is weaker than the less saturated wood. The penetration velocity is 13.6 m/sec for 30%, 13.73m/sec for 20%, 13.8 m/sec for 10%, and 14 m/sec for 1%. Thus, as the moisture content decreases, the material becomes stronger.

5 Conclusion

A 15 lb. 2"×4" rigid projectile impact on plywood composite panels has been studied by LS-DYNA for modeling the progressive failure behavior of a one single plywood composite layers. The Texas Tech University Wind Science and Engineering Research Center's study on the wind-generated missile impact on a composite wall was a major motivation on this study. Existing TTU experimental test data of 1 layer of 3/4 in plywood impacted by a 15lb 2"×4" board is used to guide and judge the finite element model development. Table 6 shows the data reported by the TTU Wind Science and Engineering Research Center. As seen from this table there is a reasonable agreement between the results of the TTU experiments and the numerical simulation. This study showed that the simulation using LS-DYNA

Table 6: Penetration velocity comparison.

Projectile Speed (m/s)	TTU Test Results	LS-DYNA Simulation Results
< 13	Projectile repercussed the target	Projectile repercussed the target
13-14	Projectile damaged the target	Projectile damaged and penetrated the target
>14	Projectile penetrated the target	The penetration of the projectile become effortless

can be used to design a safe room wall assembly.

References

[1] McPeak, B. G. and Ertas, A., 2012. The good, the bad, and the ugly facts of tornado survival. Nat Hazards 60:915935.

[2] NOAA, 2006. 2005 annual summaries. NOAA Department of Commerce, Ed.: National Climatic Data Center, pp. 36.

[3] Grazulis, T. P., 1993. Significant tornadoes 1680-1991. St. Johnsbury, VT., Environmental Films.

[4] McPeak, B. G., 2009. A transdisciplinary systems approach for defining tornado characteristics and debris impact analysis. Ph.D. Dissertation, Mechanical Engineering Departemnt, Texas Tech University, Lubbock, Texas.

[5] Wright, T.W., Frank, K.D., 1988. Approaches to penetration problems. Ballistic Research Laboratory - Aberdeen Proving Ground, Maryland.

[6] Baraff, D., 19889. Analytical methods for dynamic simulation of non-penetrating rigid bodies. ACM SIGGRAPH Computer Graphics, vol. 23, pp. 223-232.

[7] Materials response to ultra-high loading rates, 1980. Washington: National Materials Advisory Board.

[8] Anand, L., 1985. Constitutive equations for hot working of metals. Int. J. Plas., vol.1, pp. 213-232.

[9] Bammann, D. J., 1984. An internal variable model of viscoplasticity. Int. J. Engng. Sci., vol. 22, pp. 1041-1053.

[10] Curran, D.R., Seaman, L., Shockey, D.A., 1987. Dynamic failure of solids. Phys. Repts., vol. 147, pp. 253-388.

[11] Zukas, J.A., Jonas, G.H., Kimsey, K.D., Sherrick, T.M., 1981.Three dimensional impact simulation: Resources and results, in Computer analysis of large scale structures, K. C. Park, R.F. Jones, Ed. New York: ASME, pp. 35-68.

[12] Wright, T.W., Frank, K.D., 1988. Approaches to penetration problems. Ballistic Research Laboratory - Aberdeen Proving Ground, Maryland.

[13] Sun, C. T., and Chen, J.K., 1985. On the impact of initially stressed composite laminates. J.Compos.Mater, pp. 490-504.

[14] Aggour, H., and Sun., C.T., 1988. Finite element analysis of a laminated composite plate subjected to circularly distributed central impact loading. Comput.Struct., pp. 729-736.

[15] Choi, H.Y., and Chang, F.K., 1992. A model for predicting damage in graphite/epoxy laminated composites resulting from low-velocity point impact. Journal of Composite Materials, pp. 2134-2169.

[16] Chandrashekhara, K., and Schroeder, T., 1995. Nonlinear impact analysis of laminated cylindrical and doubly curved shells. J.Compos.Mater, pp. 2160-2179.

[17] Ivanov, I. I., Sadowski,T., Filipiak, M., and Knec, M., 2008. Experimental and numarical Investigation of Plywood Progressive Failure in CT Tests. Budownictwo,I Architektura , pp. 79-94.

About the Authors

Melisa Blahnik received her Bachelors in 2009 and Masters in 2010 in mechanical engineering from Texas Tech University Lubbock, TX. Melisa is currently employed as a Mechanical Design Engineer at Briggo Inc., a start-up company, in Austin Texas which makes a fully automated coffee machine kiosk.

Dr. Emrah Gumus received his B.S. in mechanical engineering in 2005 from Middle East Technical University, Ankara, Turkey. He receieved his M.S. in 2007 and his Ph.D. in 2010 from Mechanical Enginnering Department of Texas Tech University, Lubbock, TX, USA. His research interests are flexible multi-body dynamics, vibration absorbers and system identification by image processing. Currently, he is working as a senior mechanical design engineer at ASELSAN,inc., Ankara, Turkey.

Dr. Bobby G. McPeak received his BS degree in mechanical Engineering from SMU in 1983, his Master of Engineering from Texas Tech in 1999, and his PhD in Transdisciplinary Mechanical Engineering from Texas Tech in 2009. Since the age of 19, he has worked in the defense industry, except for a 5 year hiatus when he was a technical lead for the VISTA (Visible and Infrared Survey Telescope for Astronomy) telescope now commissioned in the Atacama Desert in Chile. His fascination with tornadoes actually began 4 generations ago in Tupelo, Mississippi. He is currently a systems engineer in the defense industry, an accomplished guitar player, and is writing a historical book about the 1948 McKinney tornado.

Dr. Atila Ertas is a Professor of Mechanical Engineering and Director of Transdisciplinary Ph.D. Program on Design, Process and Systems. Ertas is author/co-author of four books and co-editor of more than 35 proceedings. He has been teaching capstone design classes for more than 25 years. He is a Senior Research Fellow of the IC^2 Institute at the University of Texas Austin, a Fellow of American Society of Mechanical Engineers(ASME), a Fellow of Society for Design and Process Science (SDPS) and a Fellow and honorary member of The Academy of Transdisciplinary Learning & Advanced Studies (TheATLAS). He is also an honorary member of International Center for Transdisciplinary Research (CIRET), France. He has published over 150 scientific papers that cover many engineering technical fields. He has been PI or Co-PI on over 40 funded research projects. Under his supervision more than 180 MS and Ph.D. graduate students have received degrees.

APPENDIX

Table 2: Southern pine wood material properties with moisture content 1%.

Material Parameters based on Moisture Content of Southern Pine Wood **Moisture Content 1%** **Density 6.731E-07** **Units (kg, mm, ms, kN, Gpa)**	
Stiffness:	
EL Parallel Normal Modulus	16.72
ET Perpendicular Normal Modulus	0.9597
GLT Parallel Shear Modulus	0.8119
GLR Perpendicular Shear Modulus	0.3493
PR Parallel Major Poisson's Ratio	0.3033
Strength:	
Xt Parallel Tensile Strength	0.042590
Xc Parallel Compressive Strength	0.054760
Yt Perpendicular Tensile Strength	0.001477
Yc Perpendicular Compressive Strengt	0.010310
Sxy Parallel Shear Strength	0.009351
Syz Perpendicular Shear Strength	0.013090
Damage:	
Gf1 Parallel Fracture Energy in Tension	0.011670
Gf2 Parallel Fracture Energy in Shear	0.028480
Bfit Parallel Softening Parameter	30
Dmax Parallel Maximum Damage	0.9999
Gf1 Perpendicular Fracture Energy in Tension	0.000233
Gf2 Perpendicular Fracture Energy in Shear	0.000570
Dfit Perpendicular Softening Parameter	30
Dmax Perpendicular Maximum Damage	0.99
Hardening:	
Npar Parallel Hardening Initiation	0.5
Cpar Parallel Hardening Rate	1008
Nper Perpendicular Hardening Initiation	0.4
Cper Perpendicular Hardening Rate	252

Table 3: Southern pine wood material properties with moisture content 10%.

Material Parameters based on Moisture Content of Southern Pine Wood **Moisture Content 10%** **Density 6.731E-07** **Units (kg, mm, ms, kN, Gpa)**	
Stiffness:	
EL Parallel Normal Modulus	15.49
ET Perpendicular Normal Modulus	0.9101
GLT Parallel Shear Modulus	0.7898
GLR Perpendicular Shear Modulus	0.3323
PR Parallel Major Poisson's Ratio	0.2586
Strength:	
Xt Parallel Tensile Strength	0.066190
Xc Parallel Compressive Strength	0.037
Yt Perpendicular Tensile Strength	0.002139
Yc Perpendicular Compressive Strengt	0.007145
Sxy Parallel Shear Strength	0.008526
Syz Perpendicular Shear Strength	0.011940
Damage:	
Gf1 Parallel Fracture Energy in Tension	0.013840
Gf2 Parallel Fracture Energy in Shear	0.050160
Bfit Parallel Softening Parameter	30
Dmax Parallel Maximum Damage	0.9999
Gf1 Perpendicular Fracture Energy in Tension	0.000277
Gf2 Perpendicular Fracture Energy in Shear	0.001003
Dfit Perpendicular Softening Parameter	30
Dmax Perpendicular Maximum Damage	0.99
Hardening:	
Npar Parallel Hardening Initiation	0.5
Cpar Parallel Hardening Rate	1008
Nper Perpendicular Hardening Initiation	0.4
Cper Perpendicular Hardening Rate	252

Table 4: Southern pine wood material properties with moisture content 20%.

Material Parameters based on Moisture Content of Southern Pine Wood **Moisture Content 20%** **Density 6.731E-07** **Units (kg, mm, ms, kN, Gpa)**	
Stiffness:	
EL Parallel Normal Modulus	12.56
ET Perpendicular Normal Modulus	0.4619
GLT Parallel Shear Modulus	0.7369
GLR Perpendicular Shear Modulus	0.1655
PR Parallel Major Poisson's Ratio	0.1842
Strength:	
Xt Parallel Tensile Strength	0.052380
Xc Parallel Compressive Strength	0.018580
Yt Perpendicular Tensile Strength	0.001458
Yc Perpendicular Compressive Strengt	0.003627
Sxy Parallel Shear Strength	0.005577
Syz Perpendicular Shear Strength	0.007808
Damage:	
Gf1 Parallel Fracture Energy in Tension	0.015660
Gf2 Parallel Fracture Energy in Shear	0.046150
Bfit Parallel Softening Parameter	30
Dmax Parallel Maximum Damage	0.9999
Gf1 Perpendicular Fracture Energy in Tension	0.00313
Gf2 Perpendicular Fracture Energy in Shear	0.000923
Dfit Perpendicular Softening Parameter	30
Dmax Perpendicular Maximum Damage	0.99
Hardening:	
Npar Parallel Hardening Initiation	0.5
Cpar Parallel Hardening Rate	1008
Nper Perpendicular Hardening Initiation	0.4
Cper Perpendicular Hardening Rate	252

Table 5: Southern pine wood material properties with moisture content 30%.

Material Parameters based on Moisture Content of Southern Pine Wood **Moisture Content 30%** **Density 6.731E-07** **Units (kg, mm, ms, kN, Gpa)**	
Stiffness:	
EL Parallel Normal Modulus	11.35000
ET Perpendicular Normal Modulus	0.24680
GLT Parallel Shear Modulus	0.71520
GLR Perpendicular Shear Modulus	0.08751
PR Parallel Major Poisson's Ratio	0.15680
Strength:	
Xt Parallel Tensile Strength	0.04003
Xc Parallel Compressive Strength	0.01332
Yt Perpendicular Tensile Strength	0.00096
Yc Perpendicular Compressive Strengt	0.00257
Sxy Parallel Shear Strength	0.00428
Syz Perpendicular Shear Strength	0.00599
Damage:	
Gf1 Parallel Fracture Energy in Tension	0.02005
Gf2 Parallel Fracture Energy in Shear	0.04148
Bfit Parallel Softening Parameter	30
Dmax Parallel Maximum Damage	0.9999
Gf1 Perpendicular Fracture Energy in Tension	0.00040
Gf2 Perpendicular Fracture Energy in Shear	0.00830
Dfit Perpendicular Softening Parameter	30
Dmax Perpendicular Maximum Damage	0.99
Hardening:	
Npar Parallel Hardening Initiation	0.5
Cpar Parallel Hardening Rate	1008
Nper Perpendicular Hardening Initiation	0.4
Cper Perpendicular Hardening Ra	252